

Numerical study of alpha particle loss with toroidal field ripple based on CFETR steady-state scenario

Niuqi Li(李钮琦), Yingfeng Xu(徐颖峰), Fangchuan Zhong(钟方川), and Debing Zhang(张德兵)
Citation: Chin. Phys. B, 2024, 33 (**1**): 015202. DOI: 10.1088/1674-1056/ad03de
Journal homepage: http://cpb.iphy.ac.cn; http://iopscience.iop.org/cpb

What follows is a list of articles you may be interested in

Stability impacts from the current and pressure profile modifications within finite sized island

Yuxiang Sun(孙宇翔) and Di Hu(胡地)
Chin. Phys. B, 2023, 32 (**7**): 075212. DOI: 10.1088/1674-1056/acd369

Nonlinear mixing-based terahertz emission in inclined rippled density plasmas

K Gopal, A P Singh, and S Divya
Chin. Phys. B, 2023, 32 (**6**): 065202. DOI: 10.1088/1674-1056/aca9c9

Gyrokinetic simulation of low-*n* Alfvénic modes in tokamak HL-2A plasmas

Wen-Hao Lin(林文浩), Ji-Quan Li(李继全), J Garcia, and S Mazzi
Chin. Phys. B, 2023, 32 (**2**): 025202. DOI: 10.1088/1674-1056/ac6b23

Modeling of beam ions loss and slowing down with Coulomb collisions in EAST

Yifeng Zheng(郑艺峰), Jianyuan Xiao(肖建元), Baolong Hao(郝保龙), Liqing Xu(徐立清), Yanpeng Wang(王彦鹏), Jiangshan Zheng(郑江山), and Ge Zhuang(庄革)
Chin. Phys. B, 2022, 31 (**7**): 075201. DOI: 10.1088/1674-1056/ac5883

Numerical study of fast ion behavior in the presence of magnetic islands and toroidal field ripple in the EAST tokamak

Zhang Wei (张伟), Hu Li-Qun (胡立群), Sun You-Wen (孙有文), Ding Si-Ye (丁斯晔), Zhang Zi-Jun (张子君), Liu Song-Lin (刘松林)
Chin. Phys. B, 2014, 23 (**10**): 105201. DOI: 10.1088/1674-1056/23/10/105201

Numerical study of alpha particle loss with toroidal field ripple based on CFETR steady-state scenario

Niuqi Li(李钮琦)[1,2], Yingfeng Xu(徐颖峰)[1,2,†], Fangchuan Zhong(钟方川)[1,2], and Debing Zhang(张德兵)[3]

[1] *College of Science, Donghua University, Shanghai* 201620, *China*
[2] *Member of Magnetic Confinement Fusion Research Center, Ministry of Education, Shanghai* 201620, *China*
[3] *Department of Physics, East China University of Science and Technology, Shanghai* 200237, *China*

(Received 6 August 2023; revised manuscript received 30 September 2023; accepted manuscript online 17 October 2023)

Effects of plasma equilibrium parameters on the alpha particle loss with the toroidal field ripple based on the CFETR steady-state scenario have been numerically investigated by the orbit-following code GYCAVA. It is found that alpha particle losses decrease and loss regions become narrower with the plasma current increasing or with the magnetic field decreasing. It is because the ripple stochastic transport and the ripple well loss of alpha particle are reduced with the safety factor decreasing. Decrease of the plasma density and temperature can reduce alpha particle losses due to enhancement of the slowing-down effect. The direction of the toroidal magnetic field can significantly affect heat loads induced by lost alpha particle. The vertical asymmetry of heat loads induced by the clockwise and counter-clockwise toroidal magnetic fields are due to the fact that the ripple distribution is asymmetric about the mid-plane, which can be explained by the typical orbits of alpha particle. The maximal heat load of alpha particle for the clockwise toroidal magnetic field is much smaller than that for the counter-clockwise one.

Keywords: alpha particle loss, ripple, orbit-following, tokamak

PACS: 52.65.–y, 52.55.Fa, 96.50.Vg **DOI:** 10.1088/1674-1056/ad03de

1. Introduction

Alpha particles produced by the fusion reaction of deuterium and tritium play an important role in heating of the tokamak burning plasmas. Losses of alpha particle can destroy the plasma-facing components or the first wall of tokamak devices and can also reduce the heating efficiency of alpha particle. Some electromagnetic perturbations, which is toroidal asymmetrical, can impact the alpha particle loss significantly. The magnetic perturbation due to discreteness of the toroidal field coils can induce alpha particle losses and these lost alpha particles produce heat loads on the wall of a tokamak. Ripple losses of alpha particle have been numerically or experimentally investigated in various tokamaks, such as ITER,[1–3] TFTR,[4–9] CFETR,[10–13] and DEMO.[14]

The Chinese Fusion Engineering Test Reactor (CFETR)[15–20] is the next generation of tokamak device in the magnetically confined fusion energy development roadmap of China. Alpha particle heating is the dominant way of plasma heating[19] for the high Q burning plasmas on CFETR. Simulations of the ripple loss of alpha particle have been performed on CFETR by the orbit-following codes ORBIT[10–12] and GYCAVA.[13] Recently an orbit-following code PTC[21] has been developed for investigating the alpha particle transport and loss in CFETR or ITER burning plasmas.

We have developed a test particle code GYCAVA[22,23] based on the modern gyrokinetic theory[24] for investigating the behavior of fast particle in a tokamak. The GYCAVA code as well as the NBI code TGCO[25] have been used for studying effects of the resonant magnetic perturbations[26] and the toroidal field ripple[27] on NBI ion losses in the EAST tokamak. In our previous work, the GYCAVA code has been used to numerically study alpha particle losses with the toroidal field ripple in the CFETR steady-state[28] and hybrid[29] scenarios for different loss boundaries.[13] The numerical results show that the alpha particle loss fraction in the steady-state scenario is much larger than that in the hybrid scenario on CFETR for a large toroidal field ripple. The heat load with the first wall boundary is different from that with the LCFS boundary, which is related to transition of the lost alpha particle orbit from the ripple stochastic transport to the ripple well trapping. Therefore, the first wall is more suitable to be used as the loss boundary in alpha particle loss simulations on CFETR.

The amplitude and direction of the toroidal magnetic field and the amplitude of the current, density and temperature of plasma can impact alpha particle losses in the presence of the toroidal field ripple. Effects of these plasma equilibrium parameters on alpha particle losses with the toroidal field ripple on CFETR have not been studied in the previous work. It is of interest to investigate effects of these plasma equilibrium parameters on the ripple loss of alpha particle on CFETR in detail.

Numerical results of the alpha particle loss based on the

[†]Corresponding author. E-mail: xuyingfeng@dhu.edu.cn

© 2024 Chinese Physical Society and IOP Publishing Ltd

CFETR steady-state scenario in the presence the Coulomb collision and the toroidal field ripple simulated by the GYCAVA code are presented in this work. We focus on effects of the current, density and temperature of plasma and the toroidal magnetic field on the ripple loss of alpha particle. The guiding-center equations of motion in terms of the cylindrical coordinates were used and the first wall was used as the outer boundary in our ripple loss simulations of alpha particle.

This paper is organized as follows. Section 2 introduces the ripple effect in the GYCAVA code and simulation setup of equilibrium and ripple parameters and plasma profiles in the CFETR steady-state scenario and alpha particle sources for different plasma densities and temperatures. Section 3 gives simulation results of the alpha particle loss with the Coulomb collision and the toroidal field ripple based on the CFETR steady-state scenario for different plasma equilibrium parameters, that is, the plasma current, density and temperature and the toroidal magnetic field. Finally, Section 4 gives the summary.

2. Simulation setup

Alpha particle losses with the toroidal field ripple were studied by the guiding-center orbit-following code GYCAVA. The detail of guiding-center equations of motion including toroidal field ripple and equations related to the Coulomb collision adopted in the GYCAVA code can be seen in Ref. [13]. In order to compute alpha particle orbits outside the LCFS, the equations of motion in terms of the cylindrical coordinates (R,Z,ϕ) were used in our simulations. The magnetic field $\boldsymbol{B}$ contains the unperturbed magnetic field and toroidal ripple field. The unperturbed magnetic field $\boldsymbol{B}_0$ is toroidal axisymmetric and is expressed as

$$\boldsymbol{B}_0 = g(\psi)\nabla\phi + \nabla\phi\times\nabla\psi. \tag{1}$$

Here, ψ is the poloidal magnetic flux. In the region outside the LCFS, $g(\psi) = g(\psi_b)$. Here, ψ_b is the poloidal magnetic flux at the LCFS.

The toroidal ripple field $\delta\boldsymbol{B}^{\rm rip}$ included in the GYCAVA code is expressed as

$$\delta\boldsymbol{B}^{\rm rip} = -B_0R_0\delta(R,Z)\cos(N\phi)\nabla\phi. \tag{2}$$

Here, the ripple parameter δ is written as

$$\delta(R,Z) = \delta_0\exp\{[(R-R_{\rm rip})^2 + b_{\rm rip}Z^2]^{1/2}/w^{\rm rip}\}. \tag{3}$$

The coefficients related to toroidal field ripple of CFETR are chosen as $N = 16$, $\delta_0 = 1.57\times10^{-5}$, $R_{\rm rip} = 6.01 - 0.062Z^2$, $b_{\rm rip} = 0.021$, $w_{\rm rip} = 0.63$ m.[11,12] Figure 1(a) shows the contour lines of the toroidal field ripple δ of the CFETR tokamak. According to Eq. (3), the toroidal field ripple δ is symmetric about the plane at $Z = 0$. However, the mid-plane which is through the magnetic axis is the plane at $Z = 0.88$ m. It means that the toroidal field ripple δ is asymmetric about the mid-plane. At the same R and $|Z|$, the ripple in the region above the mid-plane is larger than that in the region below the mid-plane. The maximal value of the ripple at the LCFS is about 0.4%.

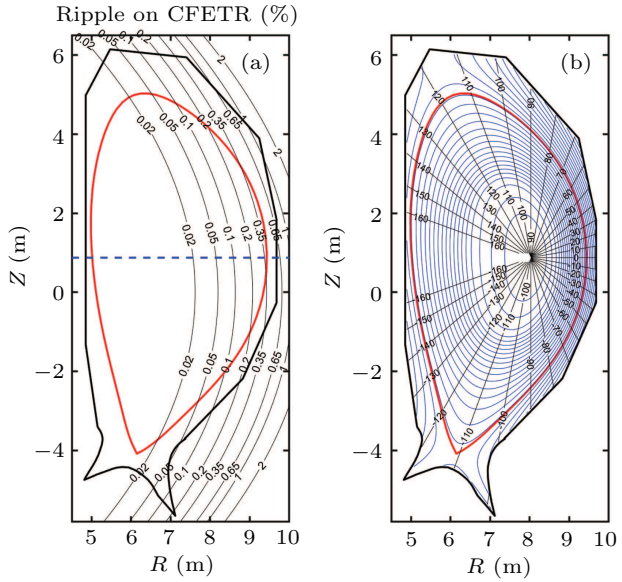


Fig. 1. (a) Contours (black line) of the toroidal field ripple and (b) contours of the poloidal magnetic flux (blue line) and the poloidal angle (black line) in the CFETR steady-state scenario. The black bold line denotes the first wall and the red bold line denotes the LCFS. The blue dash line denotes the mid-plane which is through the magnetic axis.

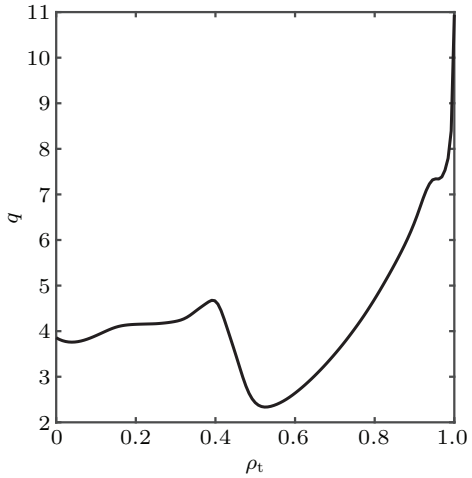


Fig. 2. The safety factor profile in the CFETR steady-state scenario.

The parameters and profiles used in our alpha particle loss simulations are based on the CFETR steady-state scenario.[28] The first wall used in our simulations is from the equilibrium data of the CFETR steady-state scenario. Some parameters in the CFETR steady-state scenario are as follows. The minor and major radii of CFETR are $a = 2.2$ m and $R_{\rm axis} = 8.0$ m, respectively. In the CFETR steady-state scenario, the unperturbed magnetic field at the axis is $B^{\rm ss}_{\rm axis} = 5.7$ T and the

plasma current is $I_{\rm p}^{\rm ss} = 11$ MA. Here, the superscript ss denotes the quantity in the CFETR steady-state scenario. Figure 1(b) shows contours of the poloidal magnetic flux and the poloidal angle in the CFETR steady-state scenario. The unperturbed magnetic field and the plasma current are both in the counterclockwise direction from the top view. The safety factor in the steady-state scenario is shown in Fig. 2. The safety factors at the magnetic axis and 95% of the poloidal magnetic flux are $q_0^{\rm ss} = 3.9$ and $q_{95}^{\rm ss} = 7.3$, respectively.

The profiles of density and temperature of electron and deuterium in the CFETR steady-state scenario, which were obtained by integrated modeling,[28] is shown in Fig. 3. The density and temperature profiles of tritium are the same as those of deuterium.

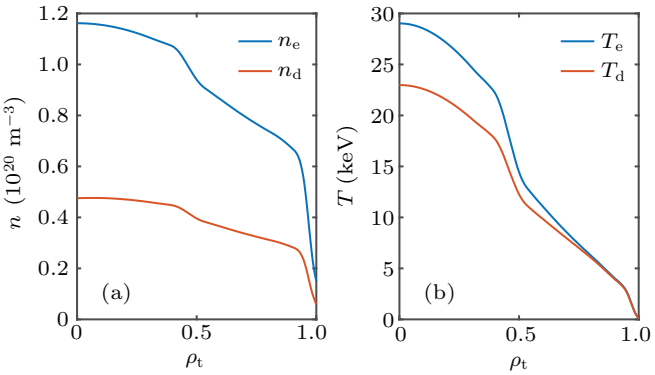


Fig. 3. The profiles of density (a) and temperature (b) of electron and deuterium in the CFETR steady-state scenario. The density and temperature profiles of tritium are the same as those of deuterium.

The initial energy of the alpha particles is $E_\alpha = 3.5$ MeV. The source or birth distribution of fusion alpha particles is computed by $S_\alpha = n_{\rm D} n_{\rm T} (\overline{\sigma v})_{\rm DT}$. Here, $(\overline{\sigma v})_{\rm DT}$ is the rate of DT fusion, which is expressed by $(\overline{\sigma v})_{\rm DT} = 3.68 \times 10^{-18} T^{-2/3} \exp(-19.94 T^{-1/3})\ {\rm m}^3 \cdot {\rm s}^{-1}$.[30,31] Here, the temperature unit T is keV. Figure 4 shows the radial birth distributions of fusion alpha particle for different density and temperature parameters (s_n and s_T). Here, $s_n = n/n^{\rm ss}$ and $s_T = T/T_{\rm ss}$ with $n^{\rm ss}$ and $T^{\rm ss}$ being the plasma density and temperature in the CFETR steady-state scenario. The source powers of alpha particle are about 9.7 MW, 180 MW, and 850 MW for $s_n = s_T = 0.5, 1, 1.5$, respectively.

The energy of an alpha particle is transferred to thermal electrons and ions by the Coulomb collision and then the alpha particle is slowed down and finally becomes a thermal ion or hit the first wall. The Coulomb collision, which contains the slowing-down effect and the pitch-angle scattering effect, is included in our ripple loss simulations of alpha particle. About twenty thousand markers are used for simulating alpha particle losses.

The radial profiles of the slowing-down time for different plasma densities and temperatures are shown in Fig. 5. We can see that the slowing-down time decreases with the s_n $(= s_T)$ decreasing or with the minor radius increasing. It is because the slowing-down time is proportional to $T_{\rm e}^{3/2}/n_{\rm e}$ and the electron density and temperature also decrease with the minor radius increasing. In the region $\rho_{\rm t} > 0.5$, the slowing-down time is smaller than 1 s. Note that the initial positions of lost alpha particle are mainly near the plasma edge. The simulation time of alpha particle loss is about 1.1 s, which is enough to make an alpha particle near the plasma edge slow down and become a thermal ion. It can also be judged by temporal evolutions of alpha particle loss in the next section.

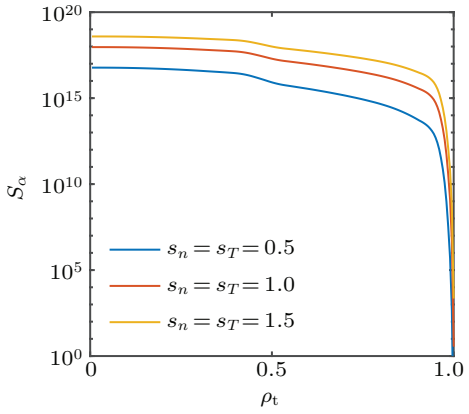


Fig. 4. Birth distributions of alpha particles in the CFETR steady-state scenario for different densities and temperatures of plasma.

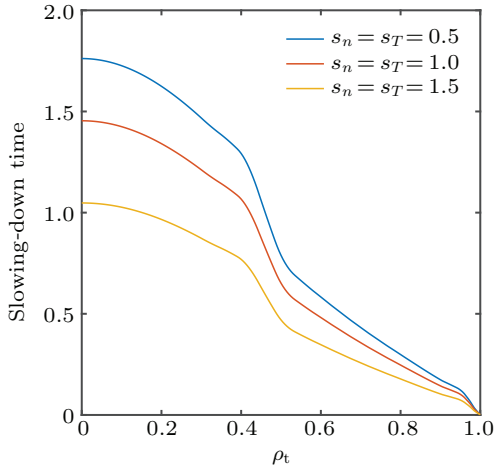


Fig. 5. The radial profiles of the slowing-down time in the CFETR steady-state scenario for different densities and temperatures of plasma.

3. Numerical results

In this section, effects of plasma equilibrium parameters on the alpha particle loss with the toroidal field ripple have been studied by scanning the amplitudes of the plasma current, density, temperature, and the toroidal magnetic field. The ripple parameter $s_\delta = \delta_0/\delta_0^{\rm cfetr}$ in our simulations is chosen as $s_\delta = 1$ or $s_\delta = 2$.

In the case with the toroidal field ripple ($s_\delta = 2$) and the Coulomb collision, a convergence study with respect to the number of markers has been done, which is shown in Fig. 6.

We can see that loss fractions of alpha particle using 20 thousand markers are within 5% of the results using more markers. In the following alpha particle loss simulations, 20 thousand markers were used.

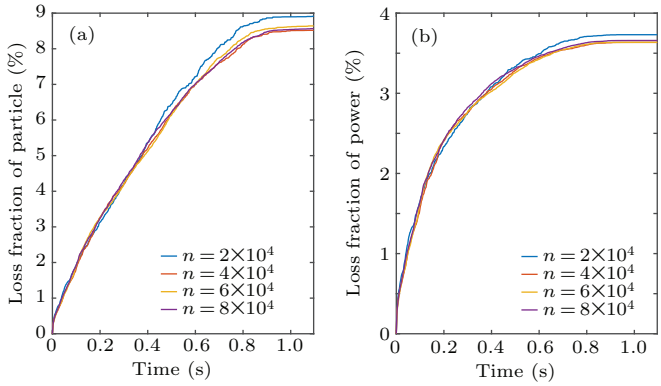


Fig. 6. Temporal evolutions of particle (a) and power (b) losses of alpha particle using different numbers of markers.

Numerical results for different plasma currents and the fixed toroidal magnetic field ($s_B = B_\phi/B_\phi^{ss} = 1$) are shown in Figs. 7–12. The relation between the alpha particle loss fractions and the plasma current with the density and temperature keeping unchanged ($s_n = s_T = 1$) is shown in Fig. 7. We can find that the particle and power losses of alpha particle decrease with the plasma current increasing in the two cases with $s_\delta = 1$ and $s_\delta = 2$. The reasons are as follows. The safety factor increases with the decreasing plasma current. The ripple stochastic diffusion effect becomes stronger with the safety factor increasing according to the theoretical criterion[32] of the ripple stochastic diffusion. In addition, increase of the safety factor make the ripple well region become wider and enhance the ripple well loss, because the ripple well region is determined by $\varepsilon/(Nq\delta) < 1$. Here, ε is the inverse aspect ratio. In the case with $s_\delta = 1$, the particle loss is about 12% for $s_I = 0.5$, which is about one order of magnitude greater than that for $s_I = 1$. Here, $s_I = I_p/I_p^{ss}$. The alpha particle losses with $s_\delta = 2$ are much larger than those with $s_\delta = 1$. It is because the ripple stochastic diffusion and the ripple well loss can be significantly enhanced by increase of the ripple parameter δ_0.

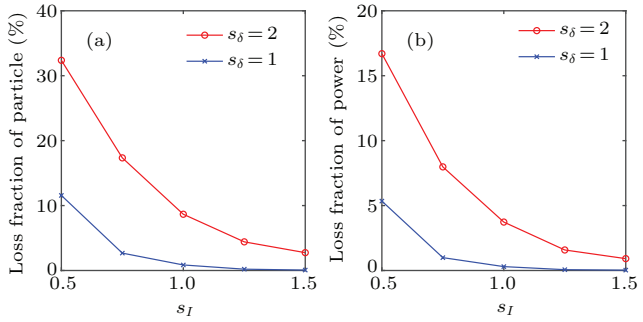


Fig. 7. Particle (a) and power (b) loss fractions of alpha particle as a function of the plasma current with $s_n = s_T = 1$. Here, $s_I = I_p/I_p^{ss}$.

Changing the plasma current with the density and temperature keeping unchanged cannot make the Grad–Shafranov equation satisfied. In order to make the plasma equilibrium still self-consistent, simulations of particle and power losses of alpha particle for different plasma currents with $s_n = s_T = s_I$ have been performed. Loss fractions, temporal evolutions, loss regions, and heat loads of alpha particles for different plasma currents and toroidal field ripples are shown in Figs. 8–12.

Loss fractions of alpha particle for different plasma currents are shown in Fig. 8. In the case with $s_I = 0.5$, the alpha particle losses with $s_n = s_T = 0.5$ are smaller than those with $s_n = s_T = 1$ shown in Fig. 7. It is related to the Coulomb collision effect. Note that the slowing-down effect of the Coulomb collision is beneficial to reduction of the alpha particle loss. From Fig. 5, we can see that the slowing-down times decreases with the decreasing density with $s_n = s_T$. Decrease of the slowing-down time means the slowing-down effect becomes stronger. Therefore, the particle and power loss fractions are reduced in the case with $s_n = s_T = 0.5$ in contrast to the case with $s_n = s_T = 1$.

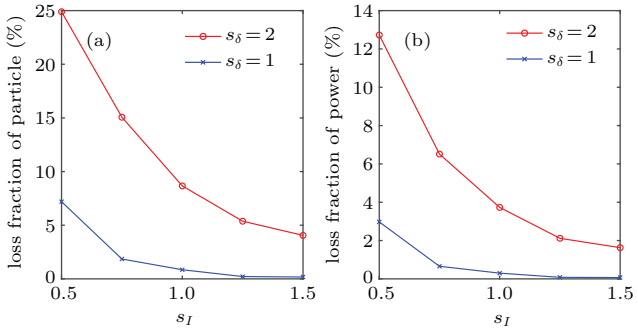


Fig. 8. Particle (a) and power (b) loss fractions of alpha particle as a function of the plasma current with $s_n = s_T = s_I$.

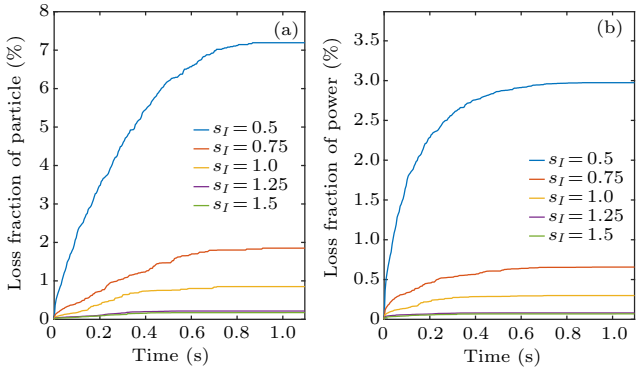


Fig. 9. Temporal evolutions of particle (a) and power (b) losses of alpha particle for different plasma currents with $s_\delta = \delta_0/\delta_0^{cfetr} = 1$ and $s_n = s_T = s_I$.

Temporal evolutions of particle and power loss of alpha particle for different plasma currents with $s_n = s_T = s_I$ and $s_\delta = 1, 2$ are shown in Figs. 9 and 10, respectively. Alpha particle losses increase with time in a long time of near 1 s in most cases. It is related to the slowing-down effect. It is found that alpha particle loss rates are rapid at the beginning and then become slowly and finally reach zero. It means that confined energetic alpha particles become thermal finally. In all our simulations, alpha particle losses in the presence of the toroidal

field ripple and the Coulomb collision reach steady states. In contrast to the case with $s_\delta = 1$ shown in Fig. 9, losses of alpha particle in the case with $s_\delta = 2$ shown in Fig. 10 are much larger because effects of the ripple stochastic diffusion and the ripple well loss become stronger with the ripple parameter increasing. The power loss rates are smaller than the particle loss rates because the energy of alpha particle included in the computation of the power loss also decreases with time due to the slowing-down effect.

Birth distributions or loss regions of lost alpha particles and their striking positions for different toroidal field ripples and plasma currents are shown in Fig. 11. Loss regions of alpha particle are mainly located at the plasma edge. In the case with $s_\delta = 1$ or $s_\delta = 2$, the loss region becomes narrower with the plasma current increasing. It is consistent with the relation between alpha particle loss fractions and the plasma current shown in Fig. 8. Loss regions in the case with $s_\delta = 2$ are much larger than those in the case with $s_\delta = 1$ for each s_I. The loss region in the case with $s_\delta = 2$ and $s_I = 0.5$ is the largest among all cases. Due to the toroidal field ripple effect, some trapped alpha particles in the core region can move outside and then strike the first wall. The pitch-angle scattering effect of the Coulomb collision can make some passing alpha particles become trapped particles, which are easily lost. Therefore, the Coulomb collision can enhance the alpha particle loss induced by the toroidal field ripple.

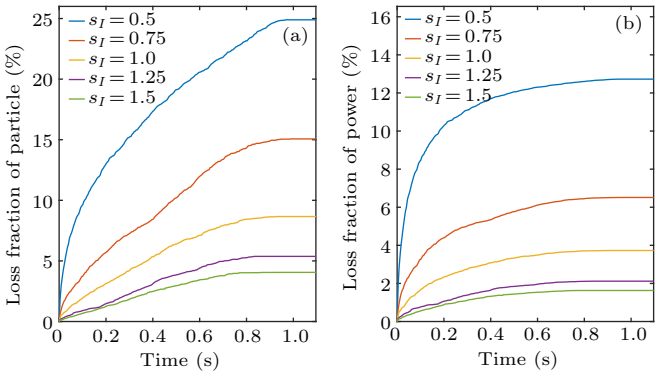


Fig. 10. Temporal evolutions of particle (a) and power (b) loss of alpha particle for different plasma currents with $s_\delta = \delta_0/\delta_0^{\rm cfetr} = 2$ and $s_n = s_T = s_I$.

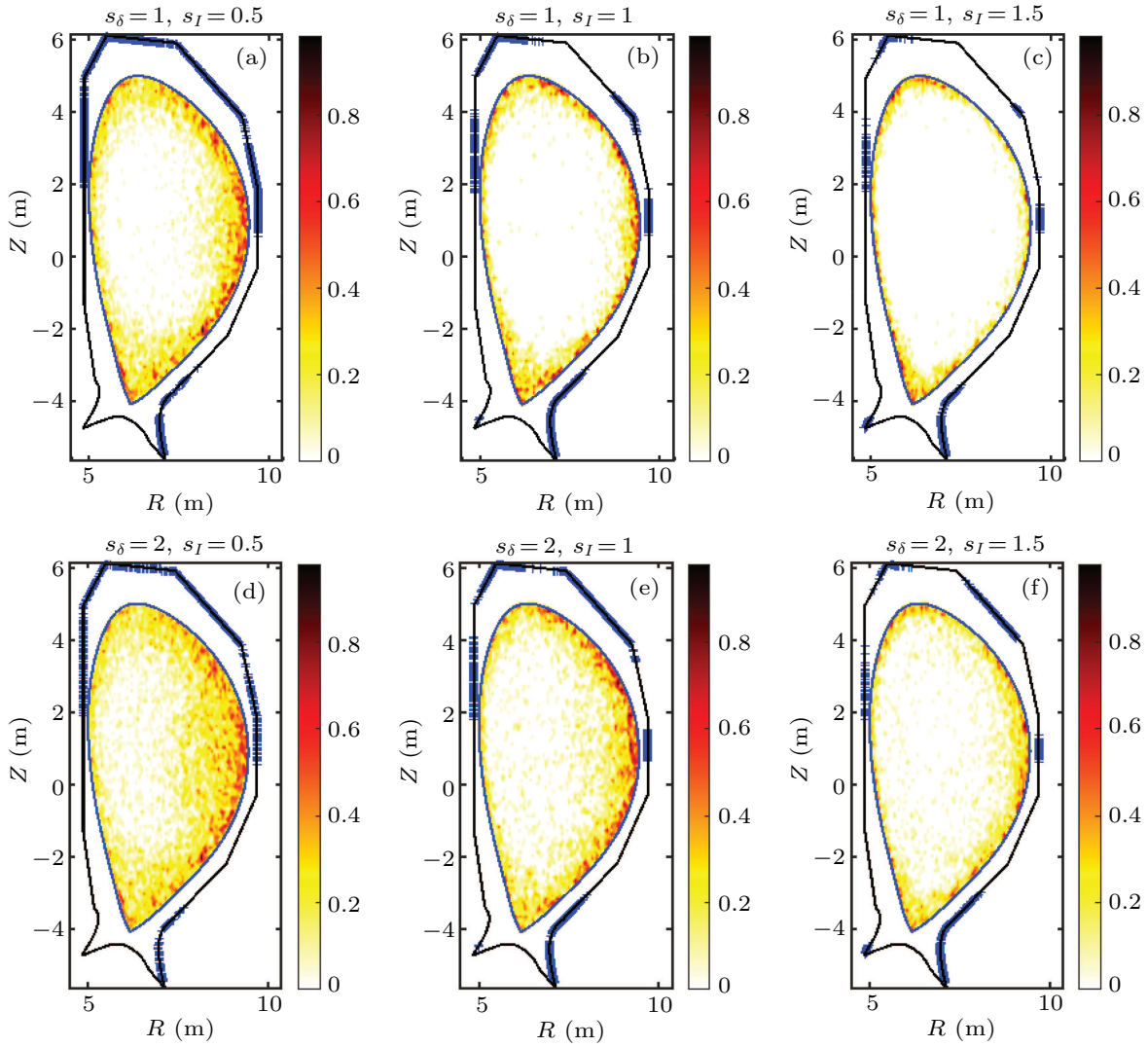


Fig. 11. Birth distributions of lost alpha particles and their striking positions (blue) for different toroidal field ripples and plasma currents with $s_n = s_T = s_I$.

Heat loads induced by lost alpha particles for different toroidal field ripples and plasma currents with $s_n = s_T = s_I$ are shown in Fig. 12. We can see that discrete hot spots located at $\theta \sim 80^\circ$ in each case. Here, θ denotes the poloidal angle. These hot spots, the number of which is the same as the number of toroidal field coils, are due to the ripple well loss. The alpha particles with a very small pitch angle in the ripple well are easily lost along the vertical direction, that is, the direction of the magnetic drift. The ripple stochastic transport and the collision-induced pitch angle scattering make more alpha particles move into the loss cone of the ripple well loss. In the case with $s_\delta = 1$ and $s_I = 1.5$, we can also find that some heat loads are located at $\theta \sim -100^\circ$, that is, the lower divertor region. The heat load is closely related to the alpha particle source power and the power loss fraction. The alpha particle source powers in the cases with $s_I = 0.5, 1, 1.5$ are 9.7 MW, 183 MW, and 850 MW, respectively. Note that $s_n = s_T = s_I$ are chosen. Heat loads due to the ripple loss are proportional to the alpha particle source powers. The power loss fraction of alpha particle, which is independent of the alpha particle source power, decreases with the plasma current increasing. It can be seen from Fig. 8(b). In the cases with $s_\delta = 1$, the maximal heat load for $s_I = 1$ is similar to that for $s_I = 1.5$. It is because both of the alpha particle source power and the loss fraction are important. In the cases with $s_\delta = 2$, the maximal heat load increases with the plasma current increasing. It is because the particle source power is dominant in these heat loads.

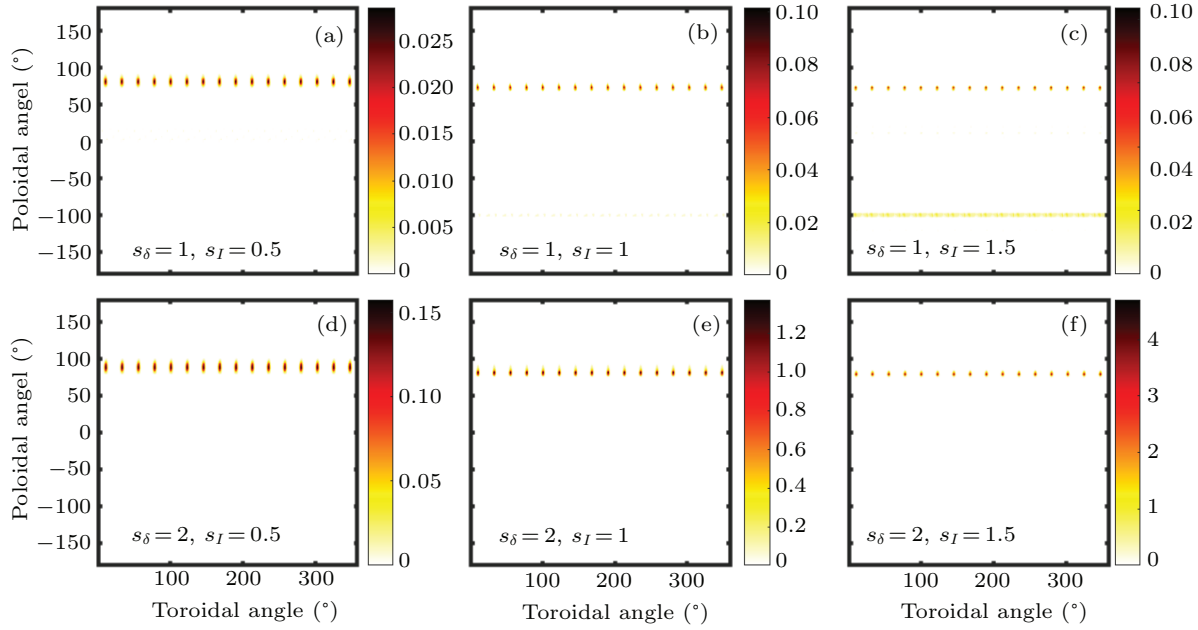


Fig. 12. Heat loads induced by lost alpha particles for different toroidal field ripples and plasma currents with $s_n = s_T = s_I$. The unit of the heat load is MW/m^2.

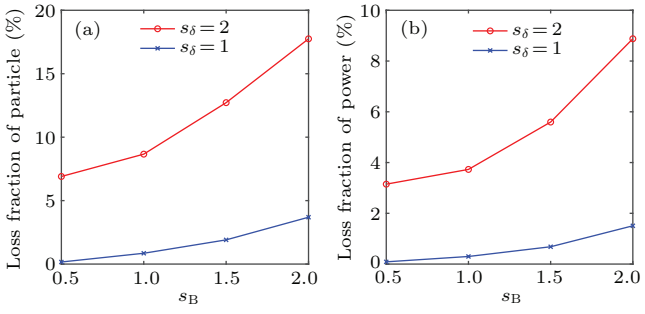


Fig. 13. Particle and power loss fractions of alpha particle as a function of the toroidal magnetic field. Here, $s_B = B_\phi / B_\phi^{ss}$.

The effect of the magnetic field on loss and heat load of alpha particle has been investigated by changing the amplitude or direction of the toroidal magnetic field. The Grad–Shafranov equation is still satisfied for different magnitude fields. In fact, the amplitude of the total magnetic field is similar to that of the toroidal magnitude field. Figure 13 shows the particle and power losses of alpha particle for different magnetic fields with $s_n = s_T = s_I = 1$. We can see that loss fractions of alpha particle increase with the magnetic field increasing. It is related to the fact that the safety factor increases with the magnetic field increasing. Increase of the safety factor enhance the ripple stochastic diffusion and the ripple well loss.

The toroidal mangetic field used in the previous simulations is in the counter-clockwise direction. In order to numerically study the impact of the toroidal magnetic field direction on the alpha particle loss, we have also simulated heat loads of alpha particle with the inverse/clockwise toroidal magnetic field, which are shown in Fig. 14. In the case with the clockwise toroidal magnetic field, the magnetic drift of an alpha particle is downward. It is found that most of heat loads are located at the region near the mid-plane, that is, the plane at $Z = 0.88$ m. It means that alpha particle losses are mainly due to the ripple stochastic transport. The ripple well loss is not

important in the cases with the inverse toroidal magnetic field. These heat load distributions are very different from the simulation results in the case with the counter-clockwise toroidal magnetic field shown in Fig. 12. We can also find that the maximal heat load for the clockwise toroidal magnetic field is much smaller than that for the counter-clockwise one in each case. It is becasue the ripple distribution is symmetric about $Z = 0$, but asymmetric about the mid-plane ($Z = 0.88$ m), which can be seen in Fig. 1(a). The ripple in the region above the mid-plane is larger than that in the region below the mid-plane at the same R and $|Z|$. It means that the ripple well loss occurs more easily in the case with the upward magnetic drift, that is, the counter-clockwise toroidal magnetic field. The vertical asymmetry of heat loads induced by the counter-clockwise and clockwise toroidal magnetic fields can also be explained by the typical orbits of alpha particle in the following. In the case with $s_\delta = 1$, heat loads are also located at the lower divertor region with the poloidal angle about $-110°$ or $-120°$. The fraction of heat load at the lower divertor increases with the plasma current increasing. In the case with $s_\delta = 2$, we can see that some heat loads are located at $\theta \sim -60°$. It is related to the vertical asymmetry of the first wall, which can be seen from a typical orbit of alpha particle in the following.

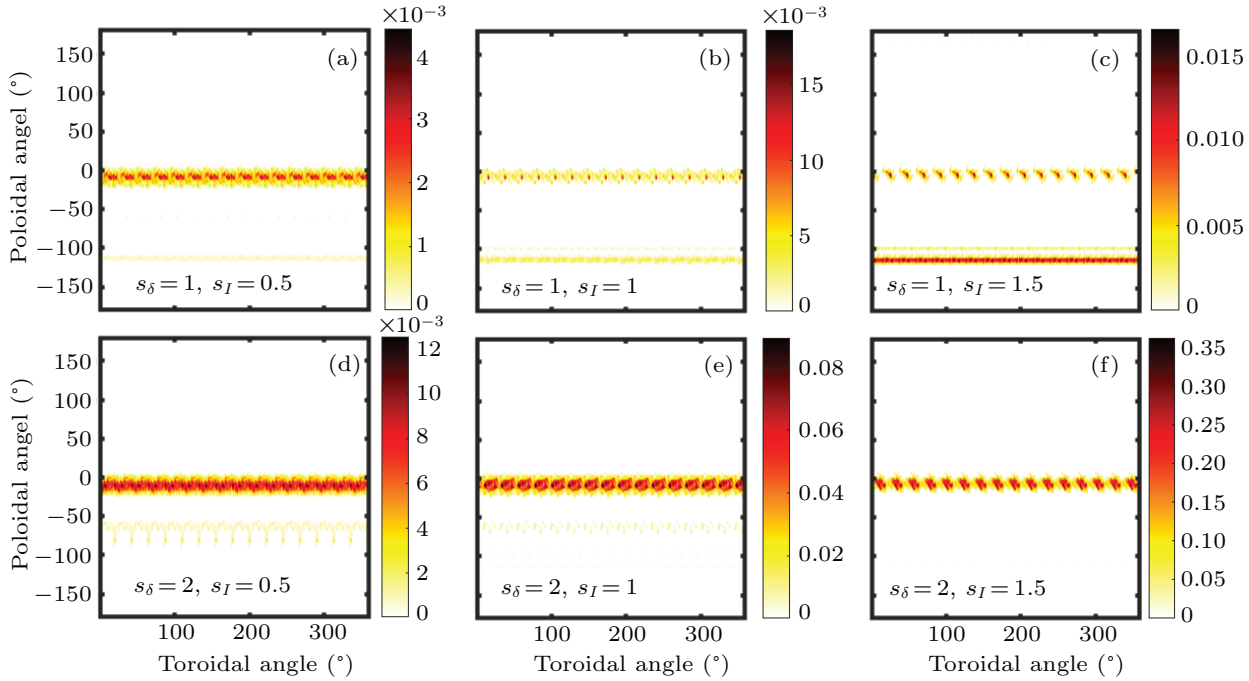


Fig. 14. Heat loads induced by lost alpha particles for the inverse direction of the toroidal magnetic field with $s_n = s_T = s_I$. The unit of the heat load is MW/m^2.

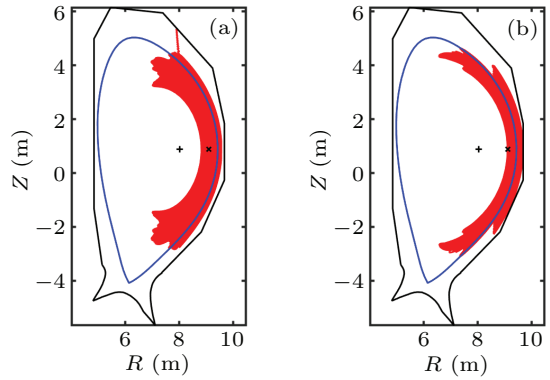


Fig. 15. Alpha particle orbits for the counter-clockwise (a) and clockwise (b) toroidal magnetic fields in the presence of the toroidal field ripple and the Coulomb collision with $\delta_0/\delta_0^{\rm cfetr} = 2$. The initial location of an alpha particle is labeled by the cross symbol and the magnetic axis is labeled by the plus symbol.

Figure 15 shows two typical alpha particle orbits for the counter-clockwise and clockwise toroidal magnetic fields in the presence of the toroidal field ripple and the Coulomb collision with the ripple parameter δ_0 chosen as $\delta_0/\delta_0^{\rm cfetr} = 2$. The initial pitch of alpha particle is $v_\parallel/v = 0.4$. In the case with the counter-clockwise toroidal magnetic field, the trapped alpha particle moves radially due to the ripple stochastic effect. We can see that the ripple field makes the turning points of the alpha particle orbit become stochastic. After the alpha particle move across the LCFS, it moves upward (in the magnetic drift direction) and then hit the first wall due to the ripple well loss mechanism. In the case with the clockwise toroidal magnetic field, the trapped alpha particle moves radially due to the ripple stochastic effect and then hit the first wall near the mid-plane. In the other words, the ripple well trapping effect is not important for the alpha orbit. It is related to vertical asymmetry of the ripple distribution about the mid-plane. The lost positions of these two typical alpha particle orbits are consistent with the main heat loads shown in Figs. 12 and 14. Due to the ver-

tical asymmetry of the first wall, we can see from Fig. 15(b) that the alpha particle orbit can be very close to the first wall at $\theta \sim -60^\circ$ in contrast to the first wall at $\theta \sim 60^\circ$. It means that some heat loads located at $\theta \sim -60^\circ$ shown in Figs. 14(d) and 14(e) are due to the vertical asymmetry of the first wall.

4. Summary

By using the GYCAVA code, effects of various plasma equilibrium parameters (the current, density, and temperature of plasma, and the toroidal magnetic field) on the alpha particle loss with the toroidal field ripple have been numerically studied based on the CFETR steady-state scenario.

Alpha particle losses decrease with the plasma current increasing or with the magnetic field decreasing, because the ripple stochastic transport and the ripple well loss of alpha particle are reduced with the safety factor decreasing. Decrease of the plasma density and temperature can reduce alpha particle losses due to enhancement of the slowing-down effect of the Coulomb collision. It is related to the fact that the slowing-down time decreases with the decreasing plasma density and temperature. Effects of the ripple stochastic diffusion and the ripple well loss become stronger with the ripple parameter increasing. Loss region of alpha particle becomes narrower with increase of the plasma current or with decrease of the magnetic field.

The direction of the toroidal magnetic field can significantly affect heat loads induced by lost alpha particles. In the cases with the counter-clockwise toroidal magnetic field, heat loads are mainly discrete hot spots on the first wall above the mid-plane, which are due to the ripple well loss. In the most cases with the clockwise toroidal magnetic field, heat loads are mainly located at the first wall near the mid-plane, which are due the ripple stochastic loss. The vertical asymmetry of heat loads induced by the counter-clockwise and clockwise toroidal magnetic fields is due to the fact that the ripple distribution is asymmetric about the mid-plane. It can be explained by typical orbits of alpha particle for the counter-clockwise and clockwise toroidal magnetic fields. The maximal heat load of alpha particle for the clockwise toroidal magnetic field is much smaller than that for the counter-clockwise one.

Acknowledgements

The authors are very grateful for the help of the CFETR team. Project supported by the National Natural Science Foundation of China (Grant Nos. 12175034 and 12005063), the National Key Research and Development Program of China (Grant No. 2019YFE03030001), and the Fundamental Research Funds for the Central Universities (Grant No. 2232022G-10).

References

[1] Tobita K, Nakayama T, Konovalov S V, *et al*. 2003 *Plasma Phys. Control. Fusion* **45** 133
[2] Shinohara K, Kurki-Suonio T, Spong D, *et al*. 2011 *Nucl. Fusion* **51** 063028
[3] Shinohara K, Tani K, Oikawa T, *et al*. 2012 *Nucl. Fusion* **52** 094008
[4] White R B and Mynick H E 1989 *Phys. Fluids B* **1** 980
[5] Darrow D S, Zweben S J, Batha S, *et al*. 1996 *Phys. Plasmas* **3** 1875
[6] Budny R V, Bell M G, Janos A C, *et al*. 1995 *Nucl. Fusion* **35** 1497
[7] Redi M H, Zarnstorff M C, White R B, *et al*. 1995 *Nucl. Fusion* **35** 1191
[8] Duong H H, Fisher R K, Medley S S, *et al*. 1997 *Nucl. Fusion* **37** 271
[9] Zweben S J, Budny R V, Darrow D S, *et al*. 2000 *Nucl. Fusion* **40** 91
[10] Hao B L, Wu B, Wang J F, *et al*. 2015 *J. Fusion Energ.* **34** 659
[11] Hao B L, Chen W, Cai H S, *et al*. 2020 *Sci. Sin-Phys. Mech. Astron.* **50** 065201
[12] Zhao R, Wang Z X, Wang F, *et al*. 2020 *Plasma Phys. Control. Fusion* **62** 115001
[13] Xu Y F, Zhang D B, Chen J L, *et al*. 2022 *Plasma Sci. Technol.* **24** 105101
[14] Pfefferlé D, Cooper W A, Fasoli A, *et al*. 2016 *Nucl. Fusion* **56** 112002
[15] Wan B N, Ding S Y, Qian J P, *et al*. 2014 *IEEE Trans. Plasma Sci.* **42** 495
[16] Song Y T, Wu S T, Li J G, *et al*. 2014 *IEEE Trans. Plasma Sci.* **42** 503
[17] Chan V S, Costley A E, Wan B N, *et al*. 2015 *Nucl. Fusion* **55** 023017
[18] Wan Y X, Li J G, Liu Y, *et al*. 2017 *Nucl. Fusion* **57** 102009
[19] Zhuang G, Li G Q, Li J, *et al*. 2019 *Nucl. Fusion* **59** 112010
[20] Gao X, Wan B N, Song Y T, *et al*. 2019 *Sci. Sin-Phys. Mech. Astron.* **49** 045202
[21] Wang F, Zhao R, Wang Z X, *et al*. 2021 *Chin. Phys. Lett.* **38** 055201
[22] Xu Y F, Guo W F, Ye L, *et al*. 2018 *Phys. Plasmas* **25** 012502
[23] Xu Y F, Guo W F, Hu Y J, *et al*. 2019 *Comput. Phys. Commun.* **244** 40
[24] Brizard A J and Hahm T S 2007 *Rev. Mod. Phys.* **79** 421
[25] Hu Y J, Xu Y F, Hao B L, *et al*. 2021 *Phys. Plasmas* **28** 122502
[26] Xu Y F, Li L, Hu Y J, *et al*. 2020 *Nucl. Fusion* **60** 086013
[27] Xu Y F, Hu Y J, Zhang X D, *et al*. 2021 *Plasma Sci. Technol.* **23** 095102
[28] Zhou C X, Chen J L, Chan V, *et al*. 2022 *Phys. Plasmas* **29** 022505
[29] Chen J L, Chan V S, Jian X, *et al*. 2021 *Nucl. Fusion* **61** 046002
[30] Huba J D 2011 *NRL Plasma Formulary* (Washington DC: Naval Research Laboratory)
[31] Ye L, Guo W F, Xiao X T, *et al*. 2014 *Phys. Plasmas* **21** 122508
[32] Goldston R J, White R B and Boozer A H 1981 *Phys. Rev. Lett.* **47** 647